

# Hybridization gap formation in the Kondo insulator YbB<sub>12</sub> observed using time-resolved photoemission spectroscopy

M. Okawa,<sup>1,2</sup> Y. Ishida,<sup>2</sup> M. Takahashi,<sup>1,\*</sup> T. Shimada,<sup>2</sup> F. Iga,<sup>3,4</sup> T. Takabatake,<sup>4</sup> T. Saitoh,<sup>1</sup> and S. Shin<sup>2,5</sup>

<sup>1</sup>*Department of Applied Physics, Tokyo University of Science, Katsushika, Tokyo 125-8585, Japan*

<sup>2</sup>*Institute for Solid State Physics, University of Tokyo, Kashiwa, Chiba 277-8581, Japan*

<sup>3</sup>*College of Science, Ibaraki University, Mito, Ibaraki 310-8512, Japan*

<sup>4</sup>*Department of Quantum Matter and Institute for Advanced Materials Research, Hiroshima University, Higashi-Hiroshima 739-8530, Japan*

<sup>5</sup>*CREST, Japan Science and Technology Agency, Chiyoda, Tokyo 102-0075, Japan*

(Dated: October 5, 2018)

A detailed low-energy electronic structure of a Kondo insulator YbB<sub>12</sub> was revealed by a synergistic combination of ultrahigh-resolution laser photoemission spectroscopy (PES) and time-resolved PES. The former confirmed a 25-meV pseudogap corresponding to the Kondo temperature of this material, and more importantly, it revealed that a 15-meV gap and a Kondo-peak feature developed below a crossover temperature  $T^* \sim 110$  K. In harmony with this, the latter discovered a very long recombination time exceeding 100 ps below  $\sim T^*$ . This is a clear manifestation of photoexcited carriers due to the bottleneck in the recovery dynamics, which is interpreted as a developing hybridization gap of a hard gap.

PACS numbers: 71.27.+a, 75.30.Mb, 79.60.-i

Due to the strong electron correlation, lanthanide and actinide  $f$  electron systems exhibit various ground states such as the Fermi liquid metal with valence fluctuation, magnetic order, quantum criticality, and exotic superconductivity. Among them, there is a class of rare-earth compounds called the Kondo insulators/semiconductors that show a metal-to-insulator crossover accompanied by a loss of local magnetic moment [1]. YbB<sub>12</sub> is a typical Kondo insulator [2, 3] with a fluctuating Yb valence around 2.9+ [4, 5]. According to infrared spectroscopy studies [6], the Drude response is sharply decreased below  $\sim 80$  K and an indirect gap of  $\sim 15$  meV opens at 8 K. Inelastic neutron scattering studies reported the spin gap of 15 meV in the insulating state [7, 8]. This crossover is frequently explained by a narrow-gap formation due to hybridization between the conduction band electrons and the localized  $f$  electrons ( $c$ - $f$  hybridization) within the scheme of the periodic Anderson model. However, there is increasing evidence that some metallic states persist within the gap of many Kondo insulators, making elusive whether the low-temperature ( $T$ ) gap is a real charge gap or a pseudogap. For example, the resistivity is still as low as  $\sim 1$   $\Omega$  cm at low  $T$  in high-quality single crystals of some Kondo insulators, such as YbB<sub>12</sub> [3] and SmB<sub>6</sub> [9]. Photoemission spectroscopy (PES) studies [10–14] reported a pseudogap feature ( $< 20$  meV) that can be interpreted as a hybridization gap, but the finite spectral weight still remained around the Fermi level  $E_F$ . In addition, tunneling spectra in YbB<sub>12</sub> exhibit that a finite state persists at the zero-bias voltage [15, 16].

In this Rapid Communication, to settle the above controversy, we investigate the electronic states within the

pseudogap as well as its evolution on cooling by an unprecedented energy resolution set to 1 meV using ultrahigh-resolution laser PES [17]. Furthermore, we employed time-resolved PES (TrPES) with a pump-probe method and investigate the nonequilibrium electron dynamics of YbB<sub>12</sub> at various temperatures. The recovery time from photoexcited nonequilibrium states is the measure of a charge gap: If there is a gap as in insulators, semiconductors, or nodeless superconductors, the electronic recovery time will become exceedingly long in comparison with a typical metal [18]. Such behavior was reported in past TrPES studies on typical semiconducting materials, such as GaAs and Si [19]. Since TrPES provides direct information of the electron-hole recombination, it is particularly appropriate to investigate such dynamics.

Single crystals of YbB<sub>12</sub> were grown by the floating zone method [3]. In both ultra-high-resolution laser PES and TrPES measurements, the samples were fractured *in situ* under the base pressure of  $\sim 2 \times 10^{-11}$  Torr, and the spectra were recorded using a VG Scienta R4000 analyzer. In ultra-high-resolution laser PES, the incident light was the sixth harmonic (6.994 eV) of a Nd:YVO<sub>4</sub> quasi-cw laser (Spectra-Physics Vanguard) [17], and the energy resolution was set to  $\Delta E = 1$ –2 meV. In TrPES, the samples were excited by a  $\sim 170$ -fs pump pulse of  $h\nu_1 = 1.47$  eV at a repetition rate of 250 kHz delivered from a Ti:sapphire amplifier (Coherent RegA 9000), and the transient was probed by  $h\nu_4 = 5.88$  eV, which is the fourth harmonic of  $h\nu_1$  generated by two  $\beta$ -BaB<sub>2</sub>O<sub>4</sub> nonlinear optical crystals [20]. To strictly avoid the multiphoton photoelectrons which start to appear at the pump fluence of  $\geq 20$   $\mu\text{J}/\text{cm}^2$ , we set it to  $\sim 15$   $\mu\text{J}/\text{cm}^2$ , which induces surface heating of  $\sim 10$  K at most, throughout the TrPES measurements. The energy and time resolutions were 12 meV and 0.41 ps, respectively, and the

\* Present address: Department of Physics, University of Tokyo, Kashiwa, Chiba 277-8561, Japan

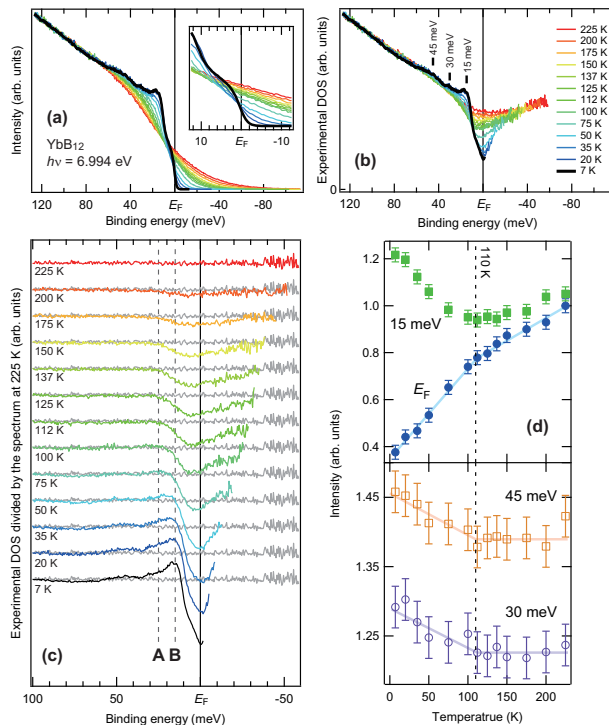


FIG. 1. Temperature dependence of the valence band spectra of  $\text{YbB}_{12}$  in the near- $E_F$  region recorded by a 7-eV laser. (a) Near- $E_F$  valence-band spectra at various temperatures. The inset shows a magnified view at  $E_F$ . (b) Experimental density of states (DOS). (c) Intensity of the experimental DOS relative to that at 225 K. (d) The spectral intensity at  $E_F$ , 15, 30, and 45 meV as functions of temperature. Solid lines are guides to the eye. Here, although the lowest temperature was in the range of 7 to 8 K, we describe it as 7 K for simplicity.

origin of pump-probe delay  $t = 0$  was calibrated *in situ* using TrPES of graphite attached next to the sample [20].  $E_F$  was calibrated using the Fermi cutoff of evaporated Au. At 6 and 35 K, we observed pump-induced surface photovoltages (SPVs) of 6.0 and 1.3 meV, respectively; We corrected the rigid photovoltaic shift of the TrPES spectra due to the SPV effect at each temperature [21].

Figure 1(a) shows temperature dependence of the ultra-high-resolution laser-PES spectra of  $\text{YbB}_{12}$ . These spectra were normalized to the area at  $110 \pm 10$  meV. We also show the experimental DOS in Fig. 1(b), which was obtained by dividing the laser-PES spectra by a Gaussian-broadened Fermi-Dirac distribution function. The spectral weight at  $E_F$  gradually decreases on cooling, reflecting the opening of a pseudogap. It is also apparent from the inset of Fig. 1(a) that the Fermi edge is present even at the lowest temperature, which is clear evidence of in-gap states coexisting with the pseudogap. A sharp peak at 15 meV and a broad peak at 45 meV were observed in the previous PES studies [13, 14]. The former corresponds to the renormalized band by the  $c$ - $f$  hybridization, whereas the latter 45-meV structure cor-

responds to the main peak of the Yb  $4f_{7/2}$  state, which can be found more clearly at 30–50 meV in hard x-ray PES spectra [5] because of a higher photoionization cross-sectional ratio [22]. In addition, we also find another small peak at 30 meV. Such fine structures observed here could be considered as the crystal-field splitting of the Yb  $4f$  state [7].

To investigate how the pseudogap and the peak develop in detail, we plot the normalized experimental DOS with respect to the 225-K DOS in Fig. 1(c). We can observe different evolutions of the two gap like features that are the large pseudogap at 25 meV [A in Fig. 1(c)] and the hybridization gap at 15 meV [B in Fig. 1(c)] on cooling; the large gap starts opening already at 200 K, the size of which is comparable with the Kondo temperature of  $\text{YbB}_{12}$ , 240 K [3]. Furthermore, the spectroscopic studies of Yb-diluted  $\text{Yb}_{1-x}\text{Lu}_x\text{B}_{12}$  reported that this pseudogap feature persists in a wide range of  $x$  [14, 23]. Therefore the large pseudogap should be attributed to the single-site Kondo effect. On the other hand, identifying the characteristic temperature of the hybridization gap is a little more complex; Fig. 1(d) shows the spectral intensity at  $E_F$ , 15, 30, and 45 meV [from Fig. 1(a)] as functions of temperature. In the upper panel of Fig. 1(d), one can observe a subtle kink in the  $E_F$  spectral weight at  $T^* \sim 110$  K, resulting in a faster depletion below  $T^*$ . Remarkably,  $T^*$  coincides with a distinct upturn of the 15-meV spectral weight that develops into a peak (upper panel) and an onset of development of the 30- and 45-meV spectral weight (lower panel) upon cooling. These facts demonstrate the hybridization-gap opening at the characteristic temperature  $T^* \sim 110$  K. We discuss this issue in depth later in terms of TrPES data.

Figures 2(a) and 2(b) show the spectral weight in the unoccupied side in the transient process, which is highlighted in a logarithmic TrPES intensity image [2(a)] and their delay profiles at  $-5$  and  $-35$  meV [2(b)]. When the pump pulse  $h\nu_1$  is irradiated at  $t = 0$ , the valence-band electrons are photoexcited, so that the spectral intensity in the occupied side decreases and tails into the unoccupied side. We observed that the high-energy ( $< -30$  meV) hot electrons relaxed into low-energy thermalized electrons through intraband transitions within  $< 1$  ps, similar to the case in a typical metal Au [24]. Nevertheless, it is apparent that the electron distribution is not completely recovered even at  $> 1$  ps, which is clearly seen as the shaded area in Fig. 2(c). This indicates that the recovery dynamics of the electronic system is bottlenecked.

To clarify the features in the anomalously long recovery, the difference spectra  $\Delta I(E_B) = I(E_B, t = 5.87 \text{ ps}) - I_{t < 0}(E_B)$  are also shown in Fig. 2(c), where  $E_B$  is the binding energy,  $I(E_B, t)$  is the PES spectrum at the delay time  $t$ , and  $I_{t < 0}(E_B)$  is the average of five spectra recorded at  $-3.46 \text{ ps} \leq t \leq -1.33 \text{ ps}$  representing the spectrum before pumping. Note, when SPV emerge at  $T < T^*$ ,  $I_{t < 0}(E_B)$  is rigidly shifted from the spectrum recorded without the pump; see later and the Supplemental Material in Ref. [21].  $\Delta I(E_B)$  exhibits

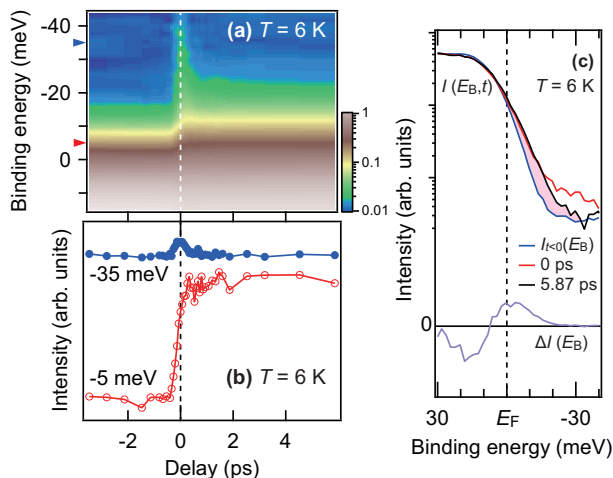


FIG. 2. (a) TrPES intensity map at 6 K as functions of binding energy and delay time with a logarithmic color scale. (b) Delay time profiles at the binding energies of  $-5$  and  $-35$  meV, corresponding to the triangles shown in panel (a). (c) TrPES spectra recorded at 6 K displayed on a logarithmic intensity scale.  $\Delta I(E_B)$  (see text) is also shown on a linear intensity scale.

a peak-and-valley feature throughout the transient, revealing the accumulation of the photoexcited electrons due to the bottleneck in the recovery dynamics. The valley bottom coincides with the 15-meV peak position observed in the valence-band spectra (Fig. 1) that should be identified as the hybridization-gap edge in the occupied side. The counterpart in the unoccupied side is the peak top located just above  $E_F$ . The hybridization gap thus does not have an electron-hole symmetry but is asymmetric regarding  $E_F$ , resulting in the gap bottom centered below  $E_F$ . This is consistent with recent infrared spectroscopy which reported an indirect hybridization-gap size of  $\sim 15$  meV [6].

It is noteworthy that the photoexcited electrons and holes do not recombine through the in-gap metallic states. Our detection of the bottlenecked electronic recovery thus has twofold implications: (i) The scattering between the states consisting of the hybridization-gap and the in-gap states is negligibly small, which will impose tight constraints on the origin of the in-gap states (discussed later); (ii) TrPES can spectroscopically identify the hybridization gap as a hard charge gap that may be buried in the in-gap states, which strongly motivates us to investigate the  $T$ -dependent dynamical response of the hybridization gap as below.

Now we discuss the temperature dependence of the transient response. We show time-dependent spectra at several temperatures between 6 and 175 K in the Supplemental Material [25]. Here, we found that the accumulation of excited electrons *gradually* weakened on warming and was hardly observed at  $T > T^* \sim 110$  K. This behavior can be explained by the fact that the photoexcited

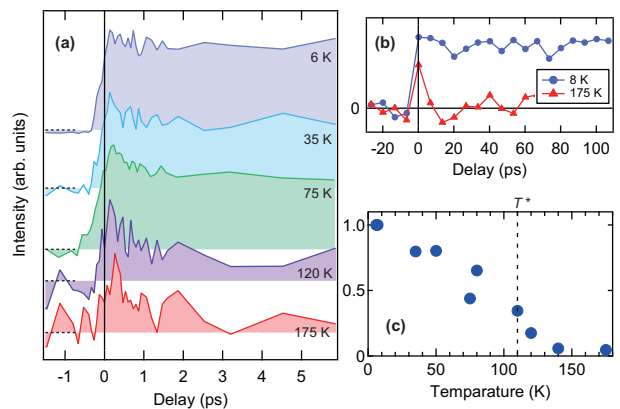


FIG. 3. (a) Time dependence of the integrated intensities in the unoccupied region ( $-45$  meV  $< E_B < E_F$ ) at several temperatures. Dashed lines correspond to the zero intensity. (b) The long range decay behaviors ( $\gg 100$  ps) at 8 and 175 K. (c) Temperature dependence of the integrated intensity between 10 and 90 ps obtained from data shown in (a). The intensities were normalized to the lowest-temperature data. The characteristic temperature ( $T^*$ ) shown in Fig. 1 is indicated by a dashed line at 110 K.

electrons rapidly go back into the occupied state via the intraband relaxation at high  $T$ , indicating the insulator-to-metal crossover with  $T$ . Since the time resolution of the TrPES measurements was  $\sim 400$  fs, such an intraband rapid relaxation could not be observed clearly. To discuss the temperature dependence of the long-lived component as a measure of the hybridization-gap formation, the spectral weight evolutions due to the accumulated electrons at 6–175 K are shown in Fig. 3(a). These are defined as the integrated intensity in the region of the unoccupied side at each temperature. The long-lived component emerges on cooling and increasingly grows below  $\sim 100$  K. As shown in Fig. 3(b), this long-lived component does not go back to the equilibrium state over 100 ps. This feature can be seen more clearly in the temperature dependence of the integrated intensity between the delay of 10 and 90 ps as shown in Fig. 3(c). Here, one can see that the long-lived component begins to be enhanced around 100–120 K upon cooling. Taking into account of the laser heating of  $\sim 10$  K, this crossover like increase in the long-lived component should correspond to  $T^* \sim 110$  K determined by the ultra-high-resolution laser-PES measurements.

Figures 4(a)–4(c) show schematics of the electron relaxation processes in metallic, crossover, and insulating (ground-state) phases. In the metallic phase ( $T \gg T^*$ ), a photoexcited electron can rapidly recombine with a hole through the intraband relaxation process. In the ground state, the  $c$ - $f$  hybridization makes a narrow and indirect gap at  $E_F$ . The long-lived component is caused by the electron-hole indirect recombination across the hybridization gap, which should be assisted by phonon or magnon scattering with a large momentum transfer

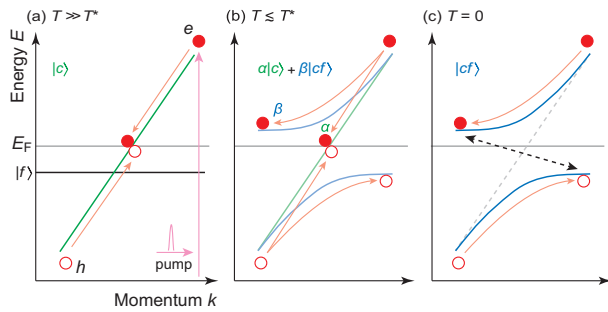


FIG. 4. Schematic electron- ( $e$ -) hole ( $h$ ) recombination processes in (a) the metallic state ( $T \gg T^*$ ), (b) the crossover state ( $T \lesssim T^*$ ), and (c) the insulating ground state ( $T = 0$ ).  $|c\rangle$ ,  $|f\rangle$ , and  $|cf\rangle$  correspond to the states of the conduction band, the localized  $f$  state, and the  $c$ - $f$  hybridized band, respectively.

[dashed arrow in Fig. 4(c)]. A computational study on the Kondo lattice model based on the nonequilibrium dynamical mean-field scheme also predicted such a long-lived feature in the Kondo-insulator limit (small- $J$  limit, where  $J$  is the Kondo coupling), being consistent with our observation [26]. Therefore,  $T^*$  can surely be interpreted as the characteristic temperature of the intrinsic hybridization-gap formation in  $\text{YbB}_{12}$ .

Another piece of evidence for the gap formation is the SPV effect: At  $T < T^*$ ,  $I_{t < 0}$  exhibited a photovoltaic shift from the spectrum recorded without a pump [21]. SPV is observed when a charge gap exists in bulk and a surface band bending develops in the surface region, a case often realized on semiconductor surfaces [27, 28]. SPV is also reported in recent TrPES studies on a Kondo insulator  $\text{SmB}_6$  [29] and a bulk insulating topological insulator  $\text{Bi}_2\text{Te}_2\text{Se}$  [30]. The carrier dynamics at  $T < T^*$  (Figs. 2 and 3) is regarded as pump-induced changes occurring in a periodic steady state realized by the irradiation of pump pulses arriving at the interval of 4  $\mu\text{s}$ .

Our method, the combination of ultra-high-resolution laser PES and TrPES, has revealed that the in-gap Fermi edge coexists with the intrinsic hybridization gap in  $\text{YbB}_{12}$ . To explain the coexistence of the hybridization-gap and the in-gap states, we consider a crossover of the two states, i.e., the nonhybridized conduction band  $|c\rangle$  and the  $c$ - $f$  hybridized band  $|cf\rangle$  [Fig. 4(b)]. Since the experiments were carried out at finite temperatures, even at the lowest one, we are practically observing the crossover state  $\alpha|c\rangle + \beta|cf\rangle$ , consisting of the high- $T$  metallic state and the insulating ground state. Therefore, there should exist two intraband decay channels of  $\alpha$  (metallic com-

ponent) and  $\beta$  (insulating component) as shown in Fig. 4(b). The gradual temperature dependence of the in-gap state [Fig. 1(d)] and the long-lived component can be interpreted as the gradual change in the probability ratio between  $|\alpha|^2$  and  $|\beta|^2$  around  $T^* \sim 110$  K.

However, the extrapolated intensity at  $E_F$  [Fig. 1(d)] towards 0 K seems to be as much as about 30% of the one at 225 K, indicating that the in-gap state exists even in the ground state. Since the experimental methods that have observed pseudogap like features of the hybridization gap in  $\text{YbB}_{12}$  (PES [10–14], including this Rapid Communication, and tunneling spectroscopy [15, 16]) are essentially surface sensitive probes, these measurements should detect the surface state to some extent. Thus we will not rule out the possibility that the observed in-gap state includes a contribution from a metallic surface. Such a metallic surface state in a band insulator creates much interest in topological insulators [31]. Recently, there have been impressive discussions on Kondo insulators  $\text{SmB}_6$ ,  $\text{YbB}_6$ , and  $\text{YbB}_{12}$  as possible three-dimensional topological insulators by both theory [32] and experiment [33]. Although the in-gap states can originate from a fractured surface quality (e.g., a surface defect state), the observed Fermi-edge state coexisting with the insulating feature in the TrPES data may meet the criteria of a topological Kondo insulator.

To summarize, the low-energy electronic structure and its transient properties of the Kondo insulator  $\text{YbB}_{12}$  were investigated using ultrahigh-resolution PES and TrPES. In the  $T$ -dependent laser-PES spectra, we found two different (pseudo)gaps with sizes of 25 and 15 meV which are attributed to the single-site effect and the insulating hybridization-gap opening, respectively. The characteristic temperature  $T^*$  was determined to be  $\sim 110$  K where the hybridization gap begins to open, although the Fermi edge remains as the in-gap state event at the lowest  $T$ . In TrPES measurements, we found that the long-lived ( $\gg 100$  ps) component gradually develops upon cooling through  $T^*$ , which is taken as a signature of the hybridization-gap evolution. Thus we experimentally determined the characteristic temperature  $T^* \sim 110$  K as the metal-to-insulator crossover in  $\text{YbB}_{12}$ .

The authors thank T. Oka, P. Werner, K. Tsunetsugu, and K. Ueda for useful discussions. This work was supported by MEXT KAKENHI Grant No. 20102004 and JSPS KAKENHI Grants No. 23540413, No. 23840039, No. 23740256, No. 25400378, No. 25420174, No. 26400321, and No. 26800165. JSPS supported this research also through the FIRST Program, initiated by the Council for Science and Technology Policy.

[1] T. Takabatake, F. Iga, T. Yoshino, Y. Echizen, K. Kato, K. Kobayashi, M. Higa, N. Shimizu, Y. Bando, G. Nakamoto, H. Fujii, K. Izawa, T. Suzuki, T. Fu-

jita, M. Sera, M. Hiroi, K. Maezawa, S. Mock, H. v. Löhneysen, A. Brückl, K. Neumaier, and K. Andres, J. Magn. Magn. Mater. **177–181**, 277 (1998); P. S. Rise-

- borough, *Adv. Phys.* **49**, 257 (2000).
- [2] M. Kasaya, F. Iga, K. Negishi, S. Nakai, and T. Kasuya, *J. Magn. Magn. Mater.* **31–34**, 437 (1983).
- [3] F. Iga, N. Shimizu, and T. Takabatake, *J. Magn. Magn. Mater.* **177–181**, 337 (1998); F. Iga, S. Hiura, J. Klijn, N. Shimizu, T. Takabatake, M. Ito, Y. Matsumoto, F. Masaki, T. Suzuki, and T. Fujita, *Physica B* **259–261**, 312 (1999).
- [4] Y. Takeda, M. Arita, M. Higashiguchi, K. Shimada, M. Sawada, H. Sato, M. Nakatake, H. Namatame, M. Taniguchi, F. Iga, T. Takabatake, Y. Takata, E. Ikenaga, M. Yabashi, D. Miwa, Y. Nishino, K. Tamasaku, T. Ishikawa, S. Shin, and K. Kobayashi, *Physica B* **351**, 286 (2004).
- [5] J. Yamaguchi, A. Sekiyama, S. Imada, H. Fujiwara, M. Yano, T. Miyamachi, G. Funabashi, M. Obara, A. Higashiya, K. Tamasaku, M. Yabashi, T. Ishikawa, F. Iga, T. Takabatake, and S. Suga, *Phys. Rev. B* **79**, 125121 (2009).
- [6] H. Okamura, S. Kimura, H. Shinozaki, T. Nanba, F. Iga, N. Shimizu, and T. Takabatake, *Phys. Rev. B* **58**, R7496 (1998); H. Okamura, T. Michikawa, T. Nanba, S.-i. Kimura, F. Iga, and T. Takabatake, *J. Phys. Soc. Jpn.* **74**, 1954 (2005).
- [7] P. A. Alekzееv, J.-M. Mignot, K. S. Nemkovski, E. V. Nefedova, N. Y. Shitsevalova, Y. B. Paderno, R. I. Bewley, R. S. Eccleston, E. S. Clementyev, V. N. Lazukov, I. P. Sadikov, and N. N. Tiden, *J. Phys.: Condens. Matter* **16**, 2631 (2004).
- [8] K. S. Nemkovski, J.-M. Mignot, P. A. Alekseev, A. S. Ivanov, E. V. Nefedova, A. V. Rybina, L.-P. Regnault, F. Iga, and T. Takabatake, *Phys. Rev. Lett.* **99**, 137204 (2007).
- [9] J. C. Cooley, M. C. Aronson, Z. Fisk, and P. C. Canfield, *Phys. Rev. Lett.* **74**, 1629 (1995).
- [10] T. Susaki, A. Sekiyama, K. Kobayashi, T. Mizokawa, A. Fujimori, M. Tsunekawa, T. Muro, T. Matsushita, S. Suga, H. Ishii, T. Hanyu, A. Kimura, H. Namatame, M. Taniguchi, T. Miyahara, F. Iga, M. Kasaya, and H. Harima, *Phys. Rev. Lett.* **77**, 4269 (1996).
- [11] T. Susaki, Y. Takeda, M. Arita, K. Mamiya, A. Fujimori, K. Shimada, H. Namatame, M. Taniguchi, N. Shimizu, F. Iga, and T. Takabatake, *Phys. Rev. Lett.* **82**, 992 (1999).
- [12] T. Susaki, A. Fujimori, Y. Takeda, M. Taniguchi, M. Arita, K. Shimada, H. Namatame, S. Hiura, F. Iga, and T. Takabatake, *J. Phys. Soc. Jpn.* **70**, 756 (2001).
- [13] Y. Takeda, M. Arita, M. Higashiguchi, K. Shimada, H. Namatame, M. Taniguchi, F. Iga, and T. Takabatake, *Phys. Rev. B* **73**, 033202 (2006).
- [14] J. Yamaguchi, A. Sekiyama, M. Y. Kimura, H. Sugiyama, Y. Tomida, G. Funabashi, S. Komori, T. Balashov, W. Wulfhekel, T. Ito, S. Kimura, A. Higashiya, K. Tamasaku, M. Yabashi, T. Ishikawa, S. Yeo, S.-I. Lee, F. Iga, T. Takabatake, and S. Suga, *New J. Phys.* **15**, 043042 (2013).
- [15] T. Ekino, H. Umeda, F. Iga, N. Shimizu, T. Takabatake, and H. Fujii, *Physica B* **259–261**, 315 (1999).
- [16] M. Bat'ková, I. Bat'ko, E. S. Konovalova, N. Shitsevalova, and Y. Paderno, *Physica B* **378–380**, 618 (2006).
- [17] T. Kiss, F. Kanetaka, T. Yokoya, T. Shimojima, K. Kanai, S. Shin, Y. Onuki, T. Togashi, C. Zhang, C. T. Chen, and S. Watanabe, *Phys. Rev. Lett.* **94**, 057001 (2005); T. Kiss, T. Shimojima, K. Ishizaka, A. Chainani, T. Togashi, T. Kanai, X.-Y. Wang, C.-T. Chen, S. Watanabe, and S. Shin, *Rev. Sci. Instrum.* **79**, 023106 (2008).
- [18] A. Rothwarf and B. N. Taylor, *Phys. Rev. Lett.* **19**, 27 (1967); J. Demsar, R. D. Averitt, A. J. Taylor, V. V. Kabanov, W. N. Kang, H. J. Kim, E. M. Choi, and S. I. Lee, *ibid.* **91**, 267002 (2003); J. Demsar, V. K. Thorsmølle, J. L. Sarrao, and A. J. Taylor, *ibid.* **96**, 037401 (2006).
- [19] J. Bokor, *Science* **246**, 1130 (1989).
- [20] Y. Ishida, T. Togashi, K. Yamamoto, M. Tanaka, T. Taniuchi, T. Kiss, M. Nakajima, T. Suemoto, and S. Shin, *Sci. Rep.* **1**, 64 (2011); Y. Ishida, T. Togashi, K. Yamamoto, M. Tanaka, T. Kiss, T. Otsu, Y. Kobayashi, and S. Shin, *Rev. Sci. Instrum.* **85**, 123904 (2014).
- [21] See the Supplemental Material at <http://dx.doi.org/10.1103/PhysRevB.92.161108> for data about emergence of SPVs.
- [22] J. J. Yeh and I. Lindau, *At. Data Nucl. Data Tables* **32**, 1 (1985).
- [23] H. Okamura, M. Matsunami, T. Inaoka, T. Nanba, S. Kimura, F. Iga, S. Hiura, J. Klijn, and T. Takabatake, *Phys. Rev. B* **62**, R13265 (2000).
- [24] W. S. Fann, R. Storz, H. W. K. Tom, and J. Bokor, *Phys. Rev. B* **46**, 13592 (1992).
- [25] See the Supplemental Material at <http://dx.doi.org/10.1103/PhysRevB.92.161108> for delay-time and temperature dependences of the near- $E_F$  spectrum as a video file.
- [26] P. Werner and M. Eckstein, *Phys. Rev. B* **86**, 045119 (2012); T. Oka and P. Werner, (private communications).
- [27] B. F. Spencer, D. M. Graham, S. J. O. Hardman, E. A. Seddon, M. J. Cliffe, K. L. Syres, A. G. Thomas, S. K. Stubbs, F. Sirotti, M. G. Silly, P. F. Kirkham, A. R. Kumarasinghe, G. J. Hirst, A. J. Moss, S. F. Hill, D. A. Shaw, S. Chattopadhyay, and W. R. Flavell, *Phys. Rev. B* **88**, 195301 (2013).
- [28] M. Ogawa, S. Yamamoto, K. Fujikawa, R. Hobara, R. Yukawa, S. Yamamoto, S. Kitagawa, D. Pierucci, M. G. Silly, C.-H. Lin, R.-Y. Liu, H. Daimon, F. Sirotti, S.-J. Tang, and I. Matsuda, *Phys. Rev. B* **88**, 165313 (2013).
- [29] Y. Ishida, T. Otsu, T. Shimada, M. Okawa, Y. Kobayashi, F. Iga, T. Takabatake, and S. Shin, *Sci. Rep.* **5**, 8160 (2015).
- [30] M. Neupane, S.-Y. Xu, Y. Ishida, S. Jia, B. M. Fregoso, C. Liu, I. Belopolski, G. Bian, N. Alidoust, T. Durakiewicz, V. Galitski, S. Shin, R. J. Cava, and M. Z. Hasan, *Phys. Rev. Lett.* **115**, 116801 (2015).
- [31] J. E. Moor, *Nature (London)* **464**, 194 (2010); M. Z. Hasan and C. L. Kane, *Rev. Mod. Phys.* **82**, 3045 (2010); Y. Ando, *J. Phys. Soc. Jpn.* **82**, 102001 (2013).
- [32] M. Dzero, K. Sun, V. Galitski, and P. Coleman, *Phys. Rev. Lett.* **104**, 106408 (2010); T. Takimoto, *J. Phys. Soc. Jpn.* **80**, 123710 (2011); F. Lu, J. Z. Zhao, H. Weng, Z. Fang, and X. Dai, *Phys. Rev. Lett.* **110**, 096401 (2013); H. Weng, J. Zhao, Z. Wang, Z. Fang, and X. Dai, *ibid.* **112**, 016403 (2014).
- [33] N. Xu, X. Shi, P. K. Biswas, C. E. Matt, R. S. Dhaka, Y. Huang, N. C. Plumb, M. Radović, J. H. Dil, E. Pomjakushina, K. Conder, A. Amato, Z. Salman, D. M. Paul, J. Mesot, H. Ding, and M. Shi, *Phys. Rev. B* **88**, 121102(R) (2013); J. Jiang, S. Li, T. Zhang, Z. Sun, F. Chen, Z. R. Ye, M. Xu, Q. Q. Ge, S. Y. Tan, X. H.

- Niu, M. Xia, B. P. Xie, Y. F. Li, X. H. Chen, H. H. Wen, and D. L. Feng, *Nat. Commun.* **4**, 3010 (2013); S. Wolgast, Ç. Kurdak, K. Sun, J. W. Allen, D.-J. Kim, and Z. Fisk, *Phys. Rev. B* **88**, 180405(R) (2013); D. J. Kim, J. Xia, and Z. Fisk, *Nature Mater.* **13**, 466 (2014); X. Zhang, N. P. Butch, P. Syers, S. Ziemak, R. L. Greene, and J. Paglione, *Phys. Rev. X* **3**, 011011 (2013); M. Neupane, N. Alidoust, S.-Y. Xu, T. Kondo, Y. Ishida, D. J. Kim, C. Liu, I. Belopolski, Y. J. Jo, T.-R. Chang, H.-T. Jeng, T. Durakiewicz, L. Balicas, H. Lin, A. Bansil, S. Shin, and M. Z. Hasan, *Nature Commun.* **4**, 2991 (2013); M. Xia, J. Jiang, Z. R. Ye, Y. H. Wang, Y. Zhang, S. D. Chen, X. H. Niu, D. F. Xu, F. Chen, X. H. Chen, B. P. Xie, T. Zhang, and D. L. Feng, *Sci. Rep.* **4**, 5999 (2014); N. Xu, C. E. Matt, E. Pomjakushina, J. H. Dil, G. Landolt, J.-Z. Ma, X. Shi, R. S. Dhaka, N. C. Plumb, M. Radovic, V. N. Strocov, T. K. Kim, M. Hoesch, K. Conder, J. Mesot, H. Ding, and M. Shi, arXiv:1405.0165.